

The Phase-Space Parameters of Brightest Halo Galaxies

Frank C. van den Bosch¹ \star , Simone M. Weinmann¹, Xiaohu Yang², H.J. Mo²,
Cheng Li³ and Y.P. Jing⁴

¹*Department of Physics, Swiss Federal Institute of Technology, ETH Hönggerberg, CH-8093, Zurich, Switzerland*

²*Department of Astronomy, University of Massachusetts, 710 North Pleasant Street, Amherst MA 01003-9305, USA*

³*Center for Astrophysics, University of Science and Technology of China, Hefei, 230026, China*

⁴*Shanghai Astronomical Observatory; the Partner Group of MPA, Nandan Road 80, Shanghai 200030, China*

ABSTRACT

The brightest galaxy in a dark matter halo is expected to reside at rest at the center of the halo. In this paper we test this ‘Central Galaxy Paradigm’ using group catalogues extracted from the Two-Degree Field Galaxy Redshift Survey (2dFGRS) and the Sloan Digital Sky Survey (SDSS). For each group we compute a parameter \mathcal{R} , which is defined as the difference between the velocity of the brightest group galaxy and the average velocity of the other group members (hereafter satellites), normalized by the unbiased estimator of the velocity dispersion of the satellite galaxies. Since the redshift surveys suffer from incompleteness effects, and the group selection criterion unavoidably selects interlopers, a proper comparison between data and model needs to take this into account. To this extent we use detailed mock galaxy redshift surveys, which are analyzed in exactly the same way as the data, thus allowing for a fair comparison. We show that the central galaxy paradigm is inconsistent with the data at high confidence, and that instead the brightest halo galaxies have a specific kinetic energy that is about 25 percent of that of the satellites. This indicates that either central galaxies reside at the minimum of the dark matter potential, but that the halo itself is not yet fully relaxed, or, that the halo is relaxed, but that the central galaxy oscillates in its potential well. The former is consistent with the fact that we find a weak hint that the velocity bias of brightest halo galaxies is larger in more massive haloes, while the latter may be indicative of cored, rather than cusped, dark matter haloes. We discuss several implications of these findings, including mass estimates based on satellite kinematics, strong gravitational lensing, halo occupation models, and the frequency and longevity of lopsidedness in disk galaxies.

Key words: galaxies: halos — galaxies: kinematics and dynamics — dark matter — methods: statistical

1 INTRODUCTION

In the standard picture of galaxy formation, hot gas in virialized dark matter haloes cools and accumulates at the center of the potential well, where it forms a galaxy (White & Rees 1978). During the hierarchical build up of larger and larger structures, haloes with their ‘central’ galaxies are accumulated by even larger haloes. At that point the halo becomes a subhalo, and the central galaxy becomes a satellite galaxy. In the standard picture, it is envisioned that a satellite galaxy no longer accretes hot gas, which instead is only accreted by the galaxy in the center of the potential well (e.g., Kauffmann, White & Guiderdoni 1993; Somerville & Primack 1999; Cole et al. 2000). Since this central galaxy

therefore continues to grow, it is expected to be the brightest, most massive galaxy in a halo. This is further assured by the fact that any other massive galaxy would quickly sink to the center of the potential well by dynamical friction to merge with the central galaxy, thus producing an even more massive central galaxy. Therefore, according to the standard paradigm, the brightest galaxy in a halo will reside at rest at the center of the potential well. Note that this is clearly a statistical statement, as it does not necessarily hold for each individual system (e.g., non-virialized, strongly interacting systems). Hereafter, we will refer to this paradigm as the ‘Central Galaxy Paradigm’ (CGP), and use the terms ‘central galaxy’ and ‘brightest halo galaxy’ without distinction.

The CGP plays an important role in various areas of astrophysics. For example, attempts to measure halo masses from the kinematics of satellite galaxies, are always based

\star E-mail: vdbosch@phys.ethz.ch

on the general assumption that the ‘host’ galaxy is located at rest at the center of a relaxed halo (e.g., Zaritsky et al. 1993, McKay et al. 2002; Brainerd & Specian 2003; Prada et al. 2003; van den Bosch et al. 2004). This assumption is also used in virtually all mass models of strong gravitational lenses. On the other hand, the observed frequency and longevity of lopsidedness in disk galaxies (e.g., Richter & Sancisi 1994; Zaritsky & Rix 1997) is often interpreted as evidence for an actual offset between galaxy and halo (e.g., Levine & Sparke 1998). The central galaxy paradigm also plays a role in halo occupation modeling, where assumptions have to be made regarding the spatial distribution of galaxies in haloes in order to compute the galaxy-galaxy correlation function on small scales (e.g., Scoccimarro et al. 2001; Berlind & Weinberg 2002; Yang, Mo & van den Bosch 2003; van den Bosch, Yang & Mo 2003; Magliocchetti & Porciani 2003; Tinker et al. 2004; Zehavi et al. 2004; Zheng et al. 2004). A statistic that is particularly sensitive to whether the brightest halo galaxies reside at the center or not is the cross correlation between dark matter haloes and galaxies (see Yang et al. 2005, in preparation).

This special dynamical status of the brightest galaxy in a halo has been tested for the special class of cD galaxies. Jones et al. (1979) have shown that cDs are located at the peak of the cluster X-ray emission, while Quintana & Lawrie (1982) used the kinematics of cluster galaxies to argue that cDs are at rest with respect to the cluster. Although this is in agreement with the CGP, more recent studies have revealed various cases in which the cD galaxy has a significant peculiar velocity with respect to the mean velocity of the other cluster members (e.g., Sharples, Ellis & Gray 1988; Hill et al. 1988; Zabludoff, Huchra & Geller 1990; Oegerle & Hill 1994, 2001). Applying a similar study to a dozen poor groups, Zabludoff & Mulchaey (1998) and Muchaey & Zabludoff (1998) found that the position of the brightest galaxy in each group is indistinguishable from that of the group center or from the center of the X-ray emission. To our knowledge, however, the central galaxy paradigm has never been tested for a statistically significant sample of dark matter haloes that span a wide range in masses. In this paper we use data from the Two-Degree Field Galaxy Redshift Survey (2dFGRS, Colless et al. 2001) and the Sloan Digital Sky Survey (SDSS; York et al. 2000) to directly test whether the brightest galaxies in dark matter haloes are located at rest at the center of their potential well. We show that, although the brightest halo galaxies are clearly segregated with respect to the other galaxies in the same halo, they have a typical specific kinetic energy that is about ~ 25 percent of that of the satellite galaxies, and that the CGP is ruled out at a high level of confidence.

This paper is organized as follows. In Section 2 we present a statistic that can be used to test the CGP, which we apply to the 2dFGRS and SDSS in Section 3. In Section 4 we describe a simple model for the velocity and spatial bias of the brightest halo galaxies, which we use in Section 5 to construct detailed mock galaxy redshift surveys of the 2dFGRS. In Section 6 we compare these mocks with the data in order to constrain the phase-space parameters of brightest halo galaxies. Section 7 discusses various implications of our results, and we summarize our conclusions in Section 8.

2 DYNAMICAL SIGNATURE OF CENTRAL GALAXIES

Observationally, the only kinematic information that is available to test the central galaxy paradigm are the line-of-sight velocities obtained from redshifts. In what follows we use v_c to refer to the line-of-sight velocity of the brightest halo galaxy, and v_i is the line-of-sight velocity of the i^{th} satellite galaxy. In addition we define the difference $\Delta V = \bar{v}_s - v_c$ between the *mean* velocity of the satellite galaxies ($\bar{v}_s = \frac{1}{N_s} \sum_{i=1}^{N_s} v_i$) and that of the central galaxy. If the CGP is correct and v_i follows a Gaussian distribution with velocity dispersion σ_s , the probability that a halo with N_s satellite galaxies has a value of ΔV is given by

$$P(\Delta V)d\Delta V = \frac{1}{\sqrt{2\pi}\sigma} \exp\left[-\frac{(\Delta V)^2}{2\sigma^2}\right] d\Delta V, \quad (1)$$

with $\sigma = \sigma_s/\sqrt{N_s}$. Therefore, in principle, one could define the parameter

$$R = \frac{\sqrt{N_s}(\bar{v}_s - v_c)}{\sigma_s}, \quad (2)$$

and test the CGP by checking whether R follows a normal distribution with zero mean and unit variance. However, the velocity dispersion σ_s is generally unknown, and we have to use its unbiased estimator

$$\hat{\sigma}_s = \sqrt{\frac{1}{N_s - 1} \sum_{i=1}^{N_s} (v_i - \bar{v}_s)^2} \quad (3)$$

instead. This allows us to define the modified parameter

$$\mathcal{R} = \frac{\sqrt{N_s}(\bar{v}_s - v_c)}{\hat{\sigma}_s}. \quad (4)$$

If the null-hypothesis of the CGP is correct, \mathcal{R} should follow a Student t -distribution with $\nu = N_s - 1$ degrees of freedom. Note that $P_\nu(\mathcal{R})$ approaches a normal distribution with zero mean and unit variance in the limit $N_s \rightarrow \infty$.

The applicability of this ‘ \mathcal{R} -test’ is strongly related to the ability to find those galaxies that belong to the same dark matter halo. To this extent we use the halo-based galaxy group finder developed by Yang et al. (2005a), which has been optimized for this task. Although this group finder is well tested and calibrated, it is not perfect. In particular, because of redshift errors and redshift space distortions, it is unavoidable that one selects interlopers (galaxies that are not associated with the same halo). The expectation value of $|v_s - v_c|$ will be larger for an interloper than for a true satellite. As long as the interloper is fainter than the brightest galaxy in the group (halo) to which it is assigned, its impact on \mathcal{R} may be small, as it affects both the numerator and the denominator. However, if the interloper is brighter than all true group members, $|\mathcal{R}|$ will typically be severely overestimated. Another problem is related to the fact that the 2dFGRS and SDSS suffer from various incompleteness effects. If the actual brightest halo galaxy is missed (i.e., is not present in the survey), \mathcal{R} will be measured with respect to a satellite galaxy, which again will bias $|\mathcal{R}|$ high. The presence of interlopers and incompleteness effects, therefore, tend to create excessive wings in the \mathcal{R} distribution. A comparison with the Student t -distribution might then give the wrong impression that the null-hypothesis is rejected. Since

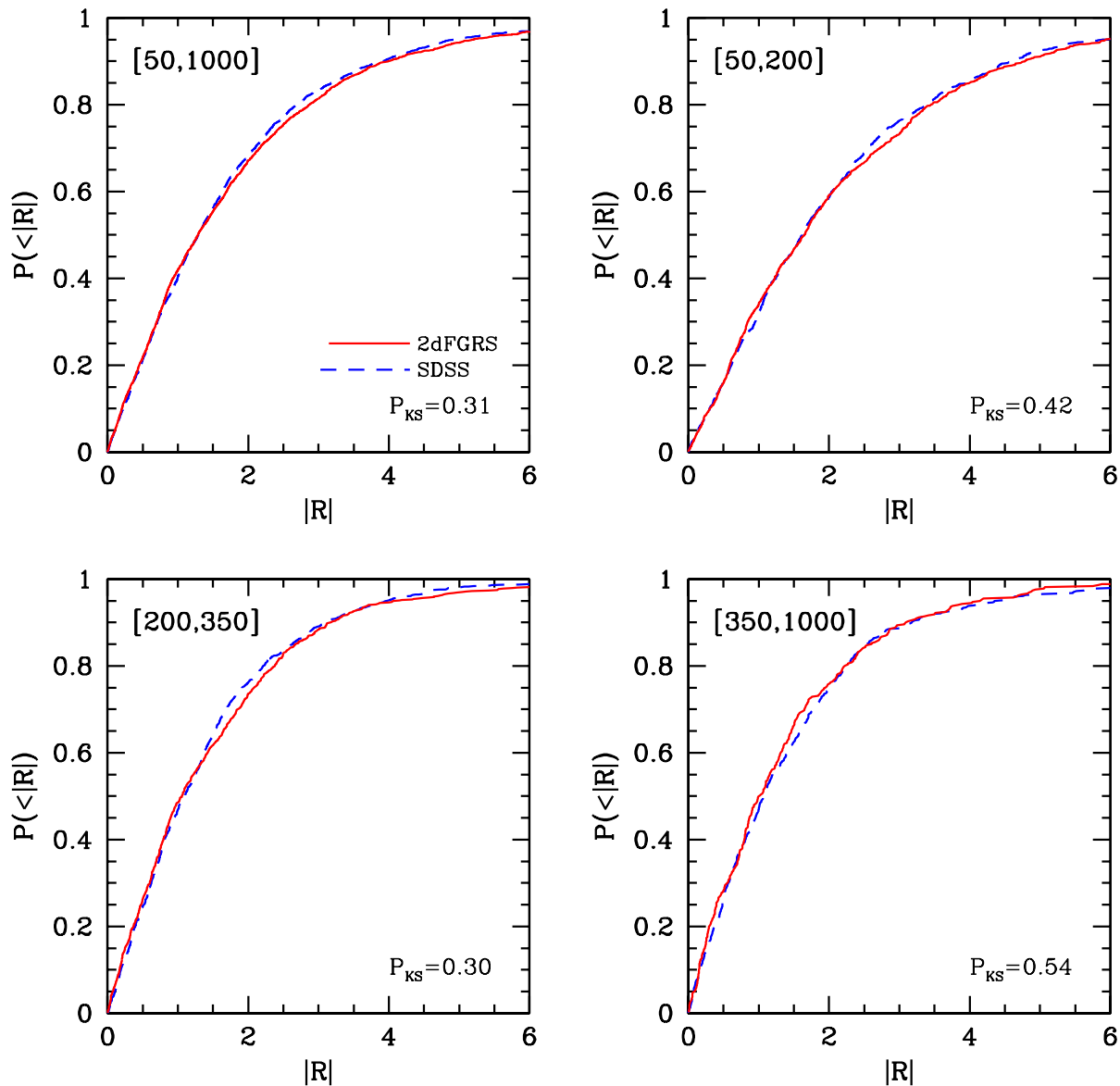


Figure 1. A comparison of the cumulative distributions of $|R|$ of 2dFGRS (red, solid lines) and SDSS (blue, dashed lines) groups. Results are shown for four intervals in $\hat{\sigma}_s$, indicated in square brackets in each panel. The KS probability, P_{KS} , that both distributions are drawn from the same distribution is also indicated. Note that the $P(|R|)$ from 2dFGRS and SDSS are in excellent agreement with each other.

the typical occupation numbers of haloes are small, this effect can be very strong, as we demonstrate in Section 6. To circumvent these problems, we compare the \mathcal{R} -distributions obtained from groups in the 2dFGRS and SDSS against those obtained from groups extracted from detailed mock galaxy redshift surveys, which suffer from interlopers and incompleteness effects to the same extent as the real data.

3 APPLICATION TO THE 2DFGRS AND SDSS

3.1 Group Selection

The \mathcal{R} -test described above requires a selection of galaxies that belong to the same dark matter halo. In Yang et al. (2005a, hereafter YMBJ) we developed a halo-based

galaxy group finder, that is optimized for this task. Here we give a brief description of this group finder, and refer the interested reader to YMBJ for details.

The basic idea behind our group finder is similar to that of the matched filter algorithm developed by Postman et al. (1996), although it also makes use of the galaxy kinematics. The group finder starts with an assumed mass-to-light ratio to assign a tentative mass to each potential group, identified using the friends-of-friends (FOF) method. This mass is used to estimate the size and velocity dispersion of the underlying halo that hosts the group, which in turn is used to determine group membership (in redshift space). This procedure is iterated until no further changes occur in group memberships. Using detailed mock galaxy redshift surveys, the performance of our group finder has been tested in terms of completeness of true members and contamination by in-

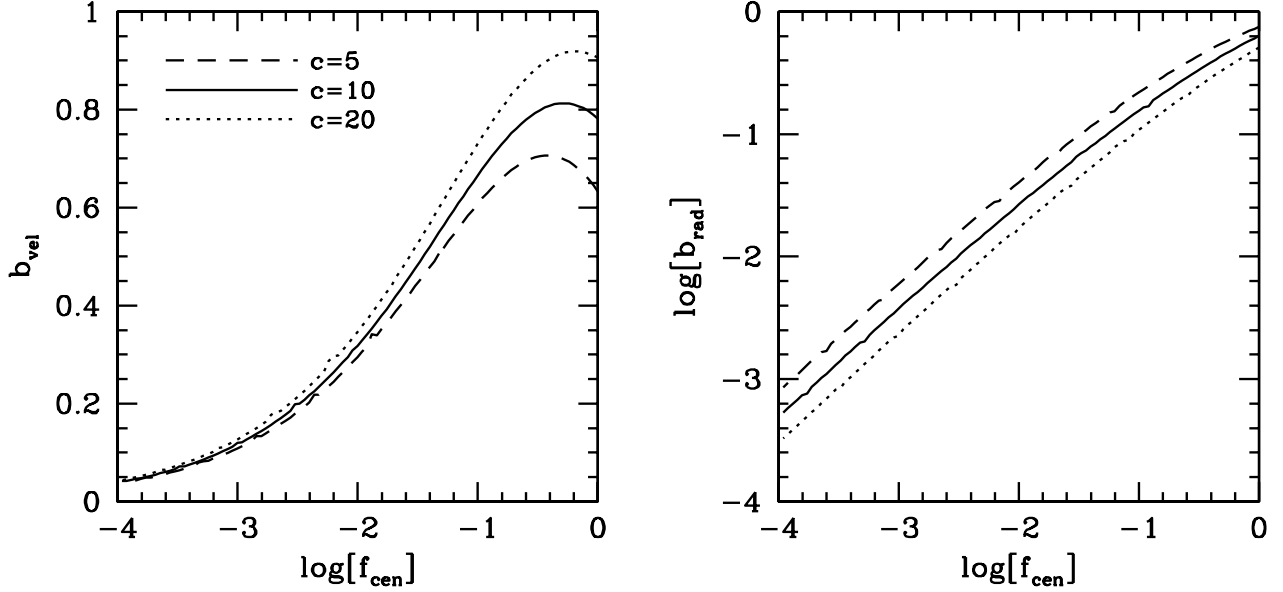


Figure 2. The velocity bias (left-hand panel) and spatial bias (right-hand panel) of central galaxies as function of the parameter f_{cen} , which expresses the characteristic scale of the radial distribution of central galaxies in terms of the characteristic scale of the NFW density distribution (see Section 4). Results are shown for three values of the halo concentration parameter c , as indicated.

terlopers. The average completeness of individual groups is ~ 90 percent and with only ~ 20 percent interlopers. Furthermore, the resulting group catalogue is insensitive to the initial assumption regarding the mass-to-light ratios, and is more successful than the conventional FOF method in associating galaxies according to their common dark matter haloes.

3.2 The 2dFGRS

We use the final, public data release from the 2dFGRS, restricting ourselves only to galaxies with redshifts $0.01 \leq z \leq 0.20$ in the North Galactic Pole and South Galactic Pole subsamples with a redshift quality parameter $q \geq 3$ and a redshift completeness $c > 0.8$. This leaves a grand total of 151,280 galaxies with a sky coverage of $\sim 1125 \text{ deg}^2$. The typical rms redshift and magnitude errors are 85 km s^{-1} and 0.15 mag, respectively (Colless et al. 2001). Absolute magnitudes for galaxies in the 2dFGRS are computed using the K-corrections of Madgwick et al. (2002).

Application of the halo-based group finder to this galaxy sample, yields a group catalogue consisting of 77,708 systems. Detailed information regarding the clustering properties and galaxy occupation statistics of these groups can be found in Yang et al. (2005a,b,c). In what follows we restrict our analyzes to the 2502 groups in this catalogue with four members or more.

3.3 The SDSS

In addition to the 2dFGRS, we also use data from the SDSS. In particular, we use the New York University Value-Added Galaxy Catalogue (NYU-VAGC)[†], described in detail in

Blanton et al. (2004). The NYU-VAGC is based on the SDSS Data Release 2 (Abazajian et al. 2004), but with an independent set of significantly improved reductions. From this catalogue we select all galaxies in the Main Galaxy Sample, which has an extinction corrected Petrosian magnitude limit of $r = 18$. We prune this sample to those galaxies in the redshift range $0.01 \leq z \leq 0.20$ and with a redshift completeness $c > 0.7$. This leaves a grand total of 184,425 galaxies with a sky coverage of $\sim 1950 \text{ deg}^2$. From this SDSS sample, we construct a group catalogue that contains 102,935 systems. A more detailed description of this catalogue will be presented in Weinmann et al. (2005, in preparation). As for the 2dFGRS, we restrict our analysis to the groups with four members or more, of which there are 3473 in our catalogue.

3.4 Comparison of 2dFGRS with SDSS

For each group in both the 2dFGRS and SDSS catalogues described above we compute \mathcal{R} . Fig. 1 plots the cumulative distributions of $|\mathcal{R}|$ for both surveys. In the upper-left panel we plot the distributions using all groups in the range $50 \text{ km s}^{-1} \leq \hat{\sigma}_s \leq 1000 \text{ km s}^{-1}$, with $\hat{\sigma}_s$ the unbiased estimator of σ_s (equation [3]). In the other three panels we plot $P(< |\mathcal{R}|)$ for three sub-samples (the values in square brackets indicate the range in $\hat{\sigma}_s$ used, in km s^{-1}). Overall the agreement between SDSS and 2dFGRS is extremely good. To make the comparison more quantitative, we use the Kolmogorov-Smirnov (hereafter KS) test to compute the probability P_{KS} that both $P(|\mathcal{R}|)$ are drawn from the same distribution. The resulting probabilities are indicated in each panel. These confirm what can already be inferred by eye, namely that both \mathcal{R} -distributions are consistent with each other. Given this good agreement between both data sets, we only concentrate on the 2dFGRS in what follows. The main reason for choosing this survey over the SDSS is that we have accurate mocks for the 2dFGRS that have been

[†] <http://wassup.physics.nyu.edu/vagc/#download>

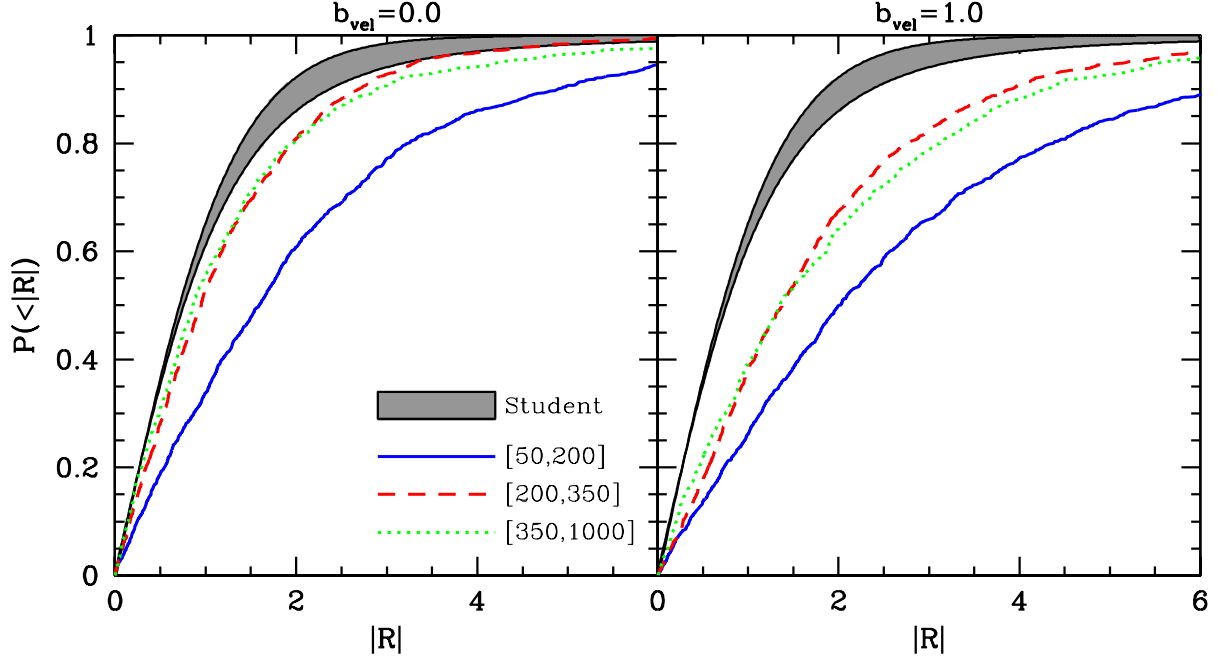


Figure 3. The cumulative distributions of $|\mathcal{R}|$ obtained from MGRSs $M_{0,0}$ (left-hand panel) and $M_{1,0}$ (right-hand panel), in which the brightest halo galaxies have a velocity bias of $b_{\text{vel}} = 0$ and $b_{\text{vel}} = 1$, respectively. Solid, dashed and dotted curves correspond to group samples with $50 \text{ km s}^{-1} \leq \hat{\sigma}_s \leq 200 \text{ km s}^{-1}$, $200 \text{ km s}^{-1} \leq \hat{\sigma}_s \leq 350 \text{ km s}^{-1}$, and $350 \text{ km s}^{-1} \leq \hat{\sigma}_s \leq 1000 \text{ km s}^{-1}$, respectively. The gray area indicates the area bounded by Student distributions with 3 and 9 degrees of freedom. In the ideal case without interlopers, the $P(< |\mathcal{R}|)$ of $M_{0,0}$ should fall in this range. The fact that they don't illustrates the impact of interlopers and completeness effects, and emphasizes the importance of using MGRSs for a fair comparison with the data. Finally, the fact that the $P(< |\mathcal{R}|)$ of $M_{0,0}$ and $M_{1,0}$ are significantly different illustrates that the \mathcal{R} -test does have the ability to constrain the phase-space parameters of brightest halo galaxies.

well tested. Given the good agreement between 2dFGRS and SDSS, we argue that any result based on the former will also hold for the latter.

4 MODELING VELOCITY BIAS OF CENTRAL GALAXIES

The main goal of this paper is to use the \mathcal{R} distributions presented above in order to constrain the phase space parameters of brightest halo galaxies. We will express these in terms of their spatial and velocity bias with respect to the satellites. If the null-hypothesis of the CGP is correct, both the spatial and the velocity bias should equal zero. In order to model these biases, and to incorporate them in the mock redshift surveys that we will use for comparison with the data, we proceed as follows.

We assume that each dark matter halo has an NFW (Navarro, Frenk & White 1997) density distribution, $\rho_{\text{dm}}(r)$, with virial radius r_{vir} , characteristic scale radius r_s , and concentration parameter $c = r_{\text{vir}}/r_s$. Assuming haloes to be spherical and isotropic, the local, one-dimensional velocity dispersion follows from solving the Jeans equation

$$\sigma_{\text{dm}}^2(r) = \frac{1}{\rho_{\text{dm}}(r)} \int_r^\infty \rho_{\text{dm}}(r') \frac{\partial \Psi}{\partial r}(r') dr' \quad (5)$$

with $\Psi(r)$ the gravitational potential (Binney & Tremaine 1987). Using that $\partial \Psi / \partial r = GM(r)/r^2$ and defining the virial velocity $V_{\text{vir}} = \sqrt{GM/r_{\text{vir}}}$ we obtain

$$\sigma_{\text{dm}}^2(r) = V_{\text{vir}}^2 \frac{c}{f(c)} \left(\frac{r}{r_s} \right) \left(1 + \frac{r}{r_s} \right)^2 \mathcal{I}(r/r_s) \quad (6)$$

with $f(x) = \ln(1+x) - x/(1+x)$ and

$$\mathcal{I}(y) = \int_y^\infty \frac{f(\tau) d\tau}{\tau^3(1+\tau)^2}. \quad (7)$$

The halo-averaged velocity dispersion is given by

$$\begin{aligned} \langle \sigma_{\text{dm}} \rangle_M &\equiv \frac{4\pi}{M} \int_0^{r_{\text{vir}}} \rho_{\text{dm}}(r) \sigma_{\text{dm}}(r) r^2 dr \\ &= V_{\text{vir}} \sqrt{\frac{c}{f^3(c)}} \int_0^c \frac{y^{3/2} \mathcal{I}^{1/2}(y)}{(1+y)} dy \end{aligned} \quad (8)$$

(cf. van den Bosch et al. 2004).

Throughout this paper, we assume that the N_{sat} satellite galaxies in a halo of mass M follow a number density distribution $n_{\text{sat}}(r) = (N_{\text{sat}}/M)\rho_{\text{dm}}(r)$, i.e., there is no spatial bias between satellite galaxies and dark matter particles. As shown in van den Bosch et al. (2005), this is consistent with the observed radial distribution of satellite galaxies in the 2dFGRS. If we further assume that the satellites are in isotropic equilibrium, it also follows that there is no velocity bias between the satellites and the dark matter, neither globally [i.e. $\langle \sigma_{\text{sat}} \rangle_M = \langle \sigma_{\text{dm}} \rangle_M$] nor locally [i.e. $\sigma_{\text{sat}}(r) = \sigma_{\text{dm}}(r)$].

When stacking all haloes of a given mass, we assume

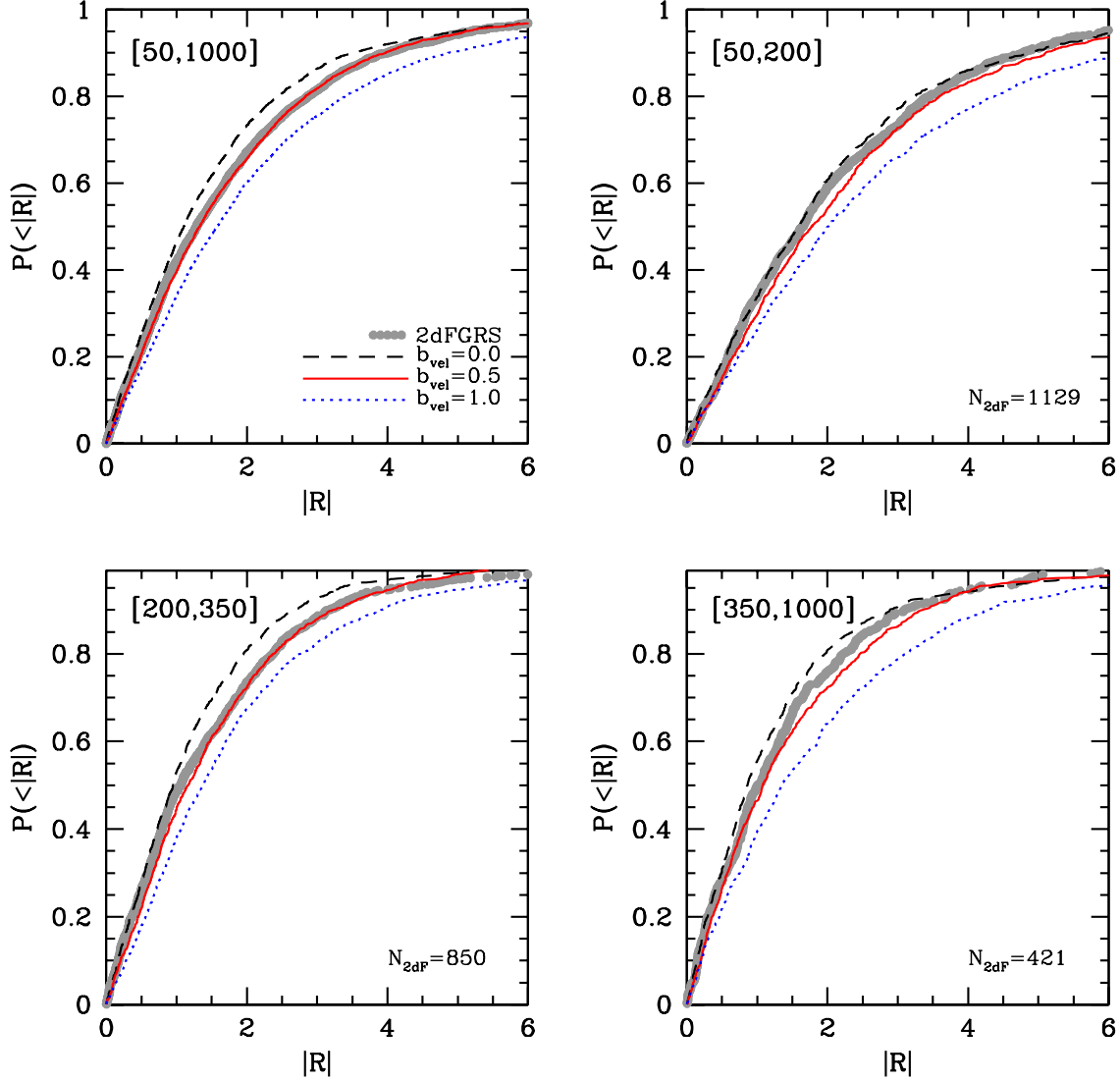


Figure 4. The cumulative distributions of $|\mathcal{R}|$ obtained from the groups in the 2dFGRS (gray dots), compared with those obtained from three of our MGRSSs, which only differ in their value of b_{vel} , as indicated in the upper left panel. Results are shown for four intervals in $\hat{\sigma}_s$, indicated in square brackets in each panel. The number of 2dF groups in each of the three subsamples is indicated.

that their brightest halo galaxies follow a number density distribution given by a Hernquist profile[‡]:

$$\rho_{\text{cen}}(r) \propto \frac{1}{2\pi} \frac{a}{r} \frac{1}{(r+a)^3} \quad (9)$$

This implies a probability distribution for r of the central galaxies of

$$P_{\text{cen}}(r)dr = 2 \left(\frac{r_{\text{vir}} + a}{r_{\text{vir}}} \right)^2 \frac{ar}{(r+a)^3} dr \quad (10)$$

In order to parameterize the characteristic radius a in terms of that of the dark matter halo, we define the parameter $f_{\text{cen}} \equiv a/r_s$. A brightest halo galaxy at a halo-centric radius

[‡] The choice for this particular distribution is not motivated by any physical considerations, other than the fact that it is well behaved, both at $r = 0$ and at $r \rightarrow \infty$

r has an isotropic velocity dispersion

$$\begin{aligned} \sigma_{\text{cen}}^2(r) &= \frac{1}{\rho_{\text{cen}}(r)} \int_r^\infty \rho_{\text{cen}}(r') \frac{\partial \Psi}{\partial r}(r') dr' \\ &= V_{\text{vir}}^2 \frac{c}{f(c)} \left(\frac{r}{r_s} \right) \left(f_{\text{cen}} + \frac{r}{r_s} \right)^3 \mathcal{J}(r/r_s), \end{aligned} \quad (11)$$

with

$$\mathcal{J}(y) = \int_y^\infty \frac{f(\tau) d\tau}{\tau^3 (f_{\text{cen}} + \tau)^3}. \quad (12)$$

This implies a halo-averaged velocity dispersion of

$$\begin{aligned} \langle \sigma_{\text{cen}} \rangle_M &\equiv \frac{\int_0^{r_{\text{vir}}} \rho_{\text{cen}}(r) \sigma_{\text{cen}}(r) r^2 dr}{\int_0^{r_{\text{vir}}} \rho_{\text{cen}}(r) r^2 dr} \\ &= V_{\text{vir}} \sqrt{\frac{4c}{f(c)}} f_{\text{cen}} \int_0^c \frac{y^{3/2} \mathcal{J}^{1/2}(y)}{(f_{\text{cen}} + y)^{3/2}} dy, \end{aligned} \quad (13)$$

which allows us to define the velocity bias of brightest halo galaxies as $b_{\text{vel}} \equiv \langle \sigma_{\text{cen}} \rangle / \langle \sigma_{\text{dm}} \rangle = \langle \sigma_{\text{cen}} \rangle / \langle \sigma_{\text{sat}} \rangle$. In addition

to the velocity bias, we define the spatial bias as $b_{\text{rad}} \equiv \langle r_{\text{cen}} \rangle / \langle r_{\text{dm}} \rangle = \langle r_{\text{cen}} \rangle / \langle r_{\text{sat}} \rangle$, where the expectation value for the radius follows from

$$\langle r \rangle = \frac{\int_0^{r_{\text{vir}}} \rho(r) r^3 dr}{\int_0^{r_{\text{vir}}} \rho(r) r^2 dr} \quad (14)$$

For an NFW density distribution with concentration c , this reduces to

$$\langle r_{\text{dm}} \rangle = \left[\frac{(2+c)/(1+c) - (2/c)\ln(1+c)}{\ln(1+c) - c/(1+c)} \right] r_{\text{vir}} \quad (15)$$

or $\langle r_{\text{dm}} \rangle = 0.41 r_{\text{vir}}$ for $c = 10$.

Fig. 2 plots b_{vel} (left-hand panel) and b_{rad} (right-hand panel) as function of f_{cen} for three values of the halo concentration parameter c . In the limit $f_{\text{cen}} \rightarrow 0$, the probability distribution $P_{\text{cen}}(r)$ becomes a Dirac delta function. This implies that the central galaxy is sitting still at the center of the dark matter halo (i.e., the null-hypothesis of the CGP), so that $b_{\text{vel}} = b_{\text{rad}} = 0$. Increasing f_{cen} increases the probability to find the brightest halo galaxy at larger halo-centric radii, which corresponds to a larger velocity bias. Note, however, that b_{vel} never approaches unity, which is due to the fact that $\rho_{\text{cen}}(r)$ can not be made to match $\rho_{\text{dm}}(r)$ for any value of f_{cen} . Typically $b_{\text{vel}} \gg b_{\text{rad}}$, which is a reflection of the ‘depth’ of the NFW potential. For example, for a velocity bias of $b_{\text{vel}} = 0.5$ (i.e., corresponding to a specific kinetic energy that is one quarter of that of the satellites) the radial bias is $b_{\text{rad}} \simeq 0.07$ (assuming $c = 10$). Combining this with (15) implies an expectation value for the offset of the central galaxy from the dark matter distribution of $\langle r_{\text{cen}} \rangle \simeq 0.03 r_{\text{vir}}$. For a Milky-Way sized system this corresponds to ~ 5 kpc, comparable to the characteristic radius (scale length) of the galaxy itself.

In what follows, we construct a set of mock galaxy redshift surveys (hereafter MGRSs) for different values of b_{vel} , and compare the \mathcal{R} -distributions of their groups against those of the 2dFGRS, which are statistically identical to those of the SDSS, in an attempt to constrain b_{vel} .

5 MOCK GALAXY REDSHIFT SURVEYS

We construct MGRSs by populating dark matter haloes with galaxies of different luminosities. The distribution of dark matter haloes is obtained from a set of large N -body simulations (dark matter only) for a Λ CDM ‘concordance’ cosmology with $\Omega_m = 0.3$, $\Omega_\Lambda = 0.7$, $h = 0.7$ and $\sigma_8 = 0.9$. In this paper we use two simulations with $N = 512^3$ particles each, which are described in more detail in Jing & Suto (2002). The simulations have periodic boundary conditions and box sizes of $L_{\text{box}} = 100h^{-1}$ Mpc (hereafter L_{100}) and $L_{\text{box}} = 300h^{-1}$ Mpc (hereafter L_{300}). We follow Yang et al. (2004) and replicate the L_{300} box on a $4 \times 4 \times 4$ grid. The central $2 \times 2 \times 2$ boxes, are replaced by a stack of $6 \times 6 \times 6$ L_{100} boxes, and the virtual observer is placed at the center (see Fig. 11 in Yang et al. 2004). This stacking geometry circumvents incompleteness problems in the mock survey due to insufficient mass resolution of the L_{300} simulations, and allows us to reach the desired depth of $z_{\text{max}} = 0.20$ in all directions.

Dark matter haloes are identified using the standard FOF algorithm with a linking length of 0.2 times the mean

inter-particle separation. Unbound haloes and haloes with less than 10 particles are removed from the sample. In Yang et al. (2004) we have shown that the resulting halo mass functions are in excellent agreement with the analytical halo mass function of Sheth, Mo & Tormen (2001).

5.1 Populating Haloes with Galaxies

In order to populate the dark matter haloes with galaxies of different luminosities, we use the conditional luminosity function (hereafter CLF), $\Phi(L|M)$, which gives the average number of galaxies of luminosity L that resides in a halo of mass M . As demonstrated in Yang, Mo & van den Bosch (2003) and van den Bosch, Yang & Mo (2003), the CLF is well constrained by the galaxy luminosity function and by the galaxy-galaxy correlation lengths as function of luminosity. In the MGRSs used here we use the CLF with ID # 6 given in Table 1 of van den Bosch et al. (2005). We have tested that none of our results depend significantly on this particular choice for the CLF.

Because of the mass resolution of the simulations and because of the completeness limit of the 2dFGRS, we adopt a minimum galaxy luminosity of $L_{\text{min}} = 10^7 h^{-2} L_\odot$. The mean number of galaxies with $L \geq L_{\text{min}}$ that resides in a halo of mass M is given by

$$\langle N \rangle_M = \int_{L_{\text{min}}}^{\infty} \Phi(L|M) dL \quad (16)$$

In order to Monte-Carlo sample occupation numbers for individual haloes, one requires the full probability distribution $P(N|M)$ (with N an integer) of which $\langle N \rangle_M$ gives the mean. We differentiate between satellite galaxies and central galaxies. The total number of galaxies per halo is the sum of N_{cen} , the number of central galaxies which is either one or zero, and N_{sat} , the (unlimited) number of satellite galaxies. We assume that N_{sat} follows a Poisson distribution and require that $N_{\text{sat}} = 0$ whenever $N_{\text{cen}} = 0$. The halo occupation distribution is thus specified as follows: if $\langle N \rangle_M \leq 1$ then $N_{\text{sat}} = 0$ and N_{cen} is either zero (with probability $P = 1 - \langle N \rangle_M$) or one (with probability $P = \langle N \rangle_M$). If $\langle N \rangle_M > 1$ then $N_{\text{cen}} = 1$ and N_{sat} is drawn from a Poisson distribution with a mean of $\langle N \rangle_M - 1$.

We follow Yang et al. (2004) and draw the luminosity of the brightest galaxy in each halo from $\Phi(L|M)$ using the restriction that $L > L_1$ with L_1 defined by

$$\int_{L_1}^{\infty} \Phi(L|M) dL = 1. \quad (17)$$

The luminosities of the satellite galaxies are also drawn from $\Phi(L|M)$, but with the restriction $L_{\text{min}} < L < L_1$.

Next we assign all galaxies a position and velocity within their halo, using the number density distributions and (isotropic) velocity dispersion profiles given in Section 4. Note that this implicitly assumes that all haloes, as well as their galaxy populations, are relaxed. Halo concentrations as function of halo mass are computed using the relation given by Eke, Navarro & Steinmetz (2001).

Table 1. Comparison between MGRSs and 2dFGRS

MGRS (1)	b_{vel} (2)	b_{rad} (3)	f_{cen} (4)	$P_{\text{KS}}[50, 1000]$ (5)	$P_{\text{KS}}[50, 200]$ (6)	$P_{\text{KS}}[200, 350]$ (7)	$P_{\text{KS}}[350, 1000]$ (8)
M _{0,0}	0.0	0.0	0.0	1.5×10^{-6}	2.6×10^{-1}	5.1×10^{-4}	2.9×10^{-2}
M _{0,1}	0.1	2.8×10^{-3}	7.3×10^{-4}	6.0×10^{-4}	8.7×10^{-1}	2.3×10^{-1}	7.4×10^{-2}
M _{0,2}	0.2	1.0×10^{-2}	3.3×10^{-3}	3.7×10^{-3}	4.9×10^{-1}	6.2×10^{-1}	8.7×10^{-2}
M _{0,3}	0.3	2.4×10^{-2}	8.5×10^{-3}	4.3×10^{-3}	4.3×10^{-1}	2.4×10^{-1}	1.6×10^{-1}
M _{0,4}	0.4	4.2×10^{-2}	1.8×10^{-2}	1.8×10^{-1}	8.2×10^{-2}	1.3×10^{-1}	3.5×10^{-1}
M _{0,5}	0.5	7.2×10^{-2}	3.5×10^{-2}	2.8×10^{-1}	7.5×10^{-2}	1.0×10^{-1}	3.8×10^{-1}
M _{0,6}	0.6	1.1×10^{-1}	6.6×10^{-2}	8.5×10^{-3}	4.0×10^{-2}	1.1×10^{-3}	1.2×10^{-1}
M _{0,7}	0.7	1.8×10^{-1}	1.3×10^{-1}	3.3×10^{-3}	3.3×10^{-3}	1.2×10^{-2}	7.0×10^{-2}
M _{0,8}	0.8	3.4×10^{-1}	3.3×10^{-1}	1.0×10^{-5}	2.4×10^{-5}	1.1×10^{-3}	7.4×10^{-3}
M _{1,0}	1.0	1.0	--	1.6×10^{-9}	1.9×10^{-5}	1.3×10^{-6}	5.3×10^{-6}

The MGRSs used for comparison with the 2dFGRS. Column (1) lists the ID of the MGRS. Columns (2), (3), and (4) list the velocity bias, spatial bias, and value of f_{cen} , respectively (see Section 4 for definitions). Finally, columns (5)–(8) list the KS probabilities P_{KS} that the distributions of \mathcal{R} extracted from these MGRS are consistent with those of the 2dFGRS for four different intervals in $\hat{\sigma}_s$, indicated by the values in square brackets (in km s^{-1}).

5.2 Creating Mock Surveys

The 2dFGRS uses a multifibre spectrograph to obtain redshifts. However, because of the physical size of the fibers, when two galaxies are closer than ~ 30 arcsec in projection only one of them can be targeted. Furthermore, due to clustering, some areas on the sky contain more galaxies within a single two-degree field than the available number of fibers. By using a sophisticated tiling strategy these problems are largely overcome, yielding a fairly uniform sampling rate. Nevertheless, some spatial non-uniformities remain. In addition, fainter galaxies yield noisier spectra, and therefore less accurate redshifts. All these effects combined result in a redshift completeness which depends on both position on the sky and on apparent magnitude. The 2dFGRS team has constructed maps that parameterize this position and magnitude dependent completeness (Colless et al. 2001; Norberg et al. 2002), and which facilitate a simulation of these effects in our MGRSs. However, as it turns out, the completeness depends also on the angular separation, θ , between galaxy *pairs* (see Hawkins et al. 2003). This is largely due to the problem of fiber collisions, which has not been completely corrected for by the tiling strategy. Finally, Norberg et al. (2002) have shown that the *parent* catalogue of the 2dFGRS, the APM catalogue, is only 91% complete. As shown in van den Bosch et al. (2005), this incompleteness is, at least partially, due to image blending in the APM catalogue (see also Cole et al. 2001). Based on this information we mimic the various observational selection and completeness effects in the 2dFGRS using the following steps:

(i) We define a (α, δ) -coordinate frame with respect to the virtual observer at the center of the stack of simulation boxes, and remove all galaxies that are not located in the areas equivalent to the NGP and SGP regions of the 2dFGRS.

(ii) For each galaxy we compute the apparent magnitude according to its luminosity and distance, to which we add a rms error of 0.15 mag. Since galaxies in the 2dFGRS were pruned by apparent magnitude *before* a K-correction was applied, we proceed as follows: We first apply a negative K-correction, then select galaxies according to the position-dependent magnitude limit (obtained using the apparent

magnitude limit masks provided by the 2dFGRS team), and finally K-correct the magnitudes back to their rest-frame b_J -band. Throughout we use the type-dependent K-corrections given in Madgwick et al. (2002).

(iii) For each galaxy we compute the redshift as ‘seen’ by the virtual observer. We take the observational velocity uncertainties into account by adding a random velocity drawn from a Gaussian distribution with dispersion 85 km s^{-1} .

(iv) To take account of the position- and magnitude-dependent completeness of the 2dFGRS, we randomly sample each galaxy using the completeness masks provided by the 2dFGRS team.

(v) To take account of the fiber-collision induced incompleteness, we compute the angular separations θ between all galaxy pairs and remove galaxies based on a probability $p(\theta)$, which we tune (by trial and error) so that we reproduce the pair-separation incompleteness quantified by Hawkins et al. (2003).

(vi) To take account of the incompleteness in the APM catalogue due to image blending we model the characteristic size of a galaxy as

$$R_{\text{gal}} = 15h^{-1} \text{ kpc} \left(\frac{L}{10^{10}h^{-2}L_{\odot}} \right)^{1/3} \quad (18)$$

and define the critical projection angle $\theta_{\text{max}} = R_{\text{gal}}/D_A$, with D_A the angular diameter distance of the galaxy. We then remove the faintest galaxy from all pairs for which $\theta < \theta_{\text{max}}$.

(vii) Finally, we remove a number of galaxies completely at random to bring the total fraction of removed galaxies, including those removed under (v) and (vi), to 9 percent.

As shown in van den Bosch et al. (2005), this procedure results in mock 2dFGRS catalogues that accurately mimic all the various incompleteness effects, allowing for a direct, one-to-one comparison with the true 2dFGRS.

6 RESULTS

Using the method outlined above, we construct a set of ten MGRSs that only differ in the value of b_{vel} . Table 1 lists these

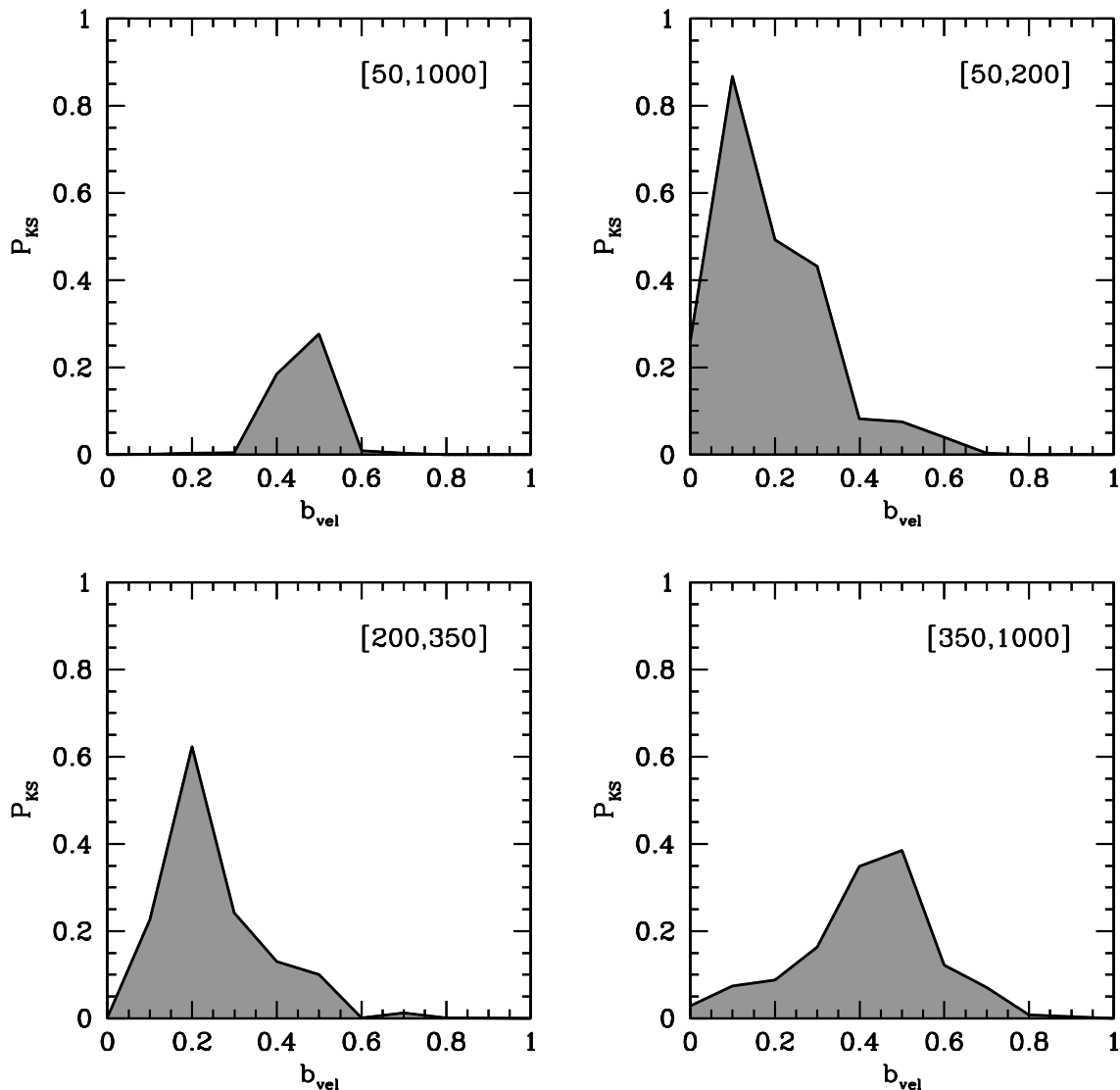


Figure 5. The KS-probability that the \mathcal{R} distribution obtained from the 2dFGRS groups is consistent with that obtained from our MGRSs, as function of b_{vel} . Results are shown for four $\hat{\sigma}_s$ -intervals, indicated in square brackets in each panel.

mocks together with their corresponding values of b_{rad} and f_{cen} , computed for a halo with a concentration parameter $c = 10$. In the case of $M_{1,0}$, we deviated somewhat from the procedure described in Section 4. Rather than giving the central galaxies a probability distribution (10), we simply treat the brightest galaxy as a satellite galaxy so that $b_{\text{vel}} = 1.0$. Note that in this case f_{cen} is not defined. For each of our ten MGRSs, we construct a group catalogue as described in Section 3.1, using those mock galaxies that are in the redshift range $0.01 \leq z \leq 0.20$ and with a completeness $c > 0.8$ (this mimics our selection from the 2dFGRS). In what follows we restrict our analysis to groups with four or more members and with $50 \text{ km s}^{-1} \leq \hat{\sigma}_s \leq 1000 \text{ km s}^{-1}$.

To illustrate the importance of using MGRSs, the left-hand panel of Fig. 3 shows the cumulative distributions of $|\mathcal{R}|$ obtained from the groups in $M_{0,0}$ for which $b_{\text{vel}} = 0.0$. In this mock all brightest halo galaxies have been located at rest at the center of the halo. The gray area indicates the area bounded by Student t -distributions with 3 and 9

degrees of freedom (corresponding to systems with 4 and 10 satellites, respectively, which spans the range covered by the vast majority of our groups). In principle, since this MGRS obeys the null-hypothesis of the CGP, the resulting $P(< |\mathcal{R}|)$ should fall in this range. Clearly it doesn't, especially not for groups with $50 \text{ km s}^{-1} \leq \hat{\sigma}_s \leq 200 \text{ km s}^{-1}$ (solid line). This owes to the completeness effects in the survey, and to the fact that our group finder is not perfect and (unavoidably) selects interlopers. As we discussed in Section 2, these effects systematically broaden $P(\mathcal{R})$ (see discussion in Section 2). Since the impact of one or two interlopers is much stronger in low mass groups, which have fewer members, the $P(\mathcal{R})$ of groups with low $\hat{\sigma}_s$ deviates more from the predicted Student t -distribution than that of more massive groups. This clearly demonstrates that one needs to take interlopers and completeness effects into account, in a statistical sense, when interpreting the distribution of \mathcal{R} obtained from the 2dFGRS. The MGRSs used here are ideally suited for this task.

The right-hand panel of Fig. 3 shows the same results as in the left-hand panel, but now based on $M_{1,0}$ for which $b_{\text{vel}} = 1.0$. Clearly, for this MGRS the $P(\mathcal{R})$ are significantly broader than for $M_{0,0}$. This demonstrates that, despite the interloper/completeness problem, the detailed distributions of \mathcal{R} obtained from group catalogues do contain useful information that we can use to constrain b_{vel} .

In Fig. 4 we compare $P(<|\mathcal{R}|)$ obtained from our 2dFGRS group catalogue (gray dots), to those obtained from three MGRSs with different values of b_{vel} , as indicated. The upper-left panel plots the results using all groups in the full range of $\hat{\sigma}_s$ considered. Clearly, the MGRS with $b_{\text{vel}} = 0.0$ (i.e. the one that fulfills the null-hypothesis of the CGP) predicts a narrower distribution of $|\mathcal{R}|$ than that found for the 2dFGRS. Although a model in which there is absolutely no segregation of the brightest galaxy, i.e., $b_{\text{vel}} = 1.0$, predicts a distribution that is clearly too broad, the intermediate case, with $b_{\text{vel}} = 0.5$ matches the 2dFGRS results nicely. Similar, though somewhat more noisy results (because of the smaller number of groups involved) are obtained for the three separate bins of $\hat{\sigma}_s$ shown in the other three panels.

Fig. 5 plots the KS probability, P_{KS} , that the $P(|\mathcal{R}|)$ of the 2dFGRS and the MGRS are drawn from the same distribution, as function of b_{vel} (see also Table 1). This analysis shows that the brightest halo galaxies in the 2dFGRS (and thus also the SDSS) have a non-zero velocity with respect to the coordinate frame in which the mean satellite motion is zero. When using all groups in the range $50 \text{ km s}^{-1} \leq \hat{\sigma}_s \leq 1000 \text{ km s}^{-1}$, the data is most consistent with a velocity bias of $b_{\text{vel}} \simeq 0.5$, while the null hypothesis of the CGP is rejected at a high level of confidence ($P_{\text{KS}} = 1.5 \times 10^{-6}$, cf. Table 1). When analyzing the three $\hat{\sigma}_s$ -subsamples, there is a hint that the velocity bias of brightest halo galaxies is more pronounced in more massive haloes. We caution, however, that these results are more noisy due to the smaller number statistics.

7 DISCUSSION

Our finding that brightest halo galaxies have, on average, a specific kinetic energy that is ~ 25 percent of that of satellite galaxies has two possible interpretations. First of all, the central galaxy may not be at rest with respect to the *virialized* dark matter halo. This scenario, which we hereafter refer to as the Non-Relaxed Galaxy (NRG) scenario, is illustrated in the left-hand panel of Fig. 6. The right-hand panel depicts the second possible scenario; that of a Non-Relaxed Halo (NRH). In this case, the brightest halo galaxy is located at rest with respect to the *minimum* of the dark matter potential, but the dark matter mass distribution is not relaxed and reveals a clear $m = 1$ mode (i.e., the potential minimum does not coincide with the barycenter). In both scenarios, the brightest halo galaxy has a net velocity with respect to the coordinate frame defined by the mean motion of the satellites. Note that, although our MGRSs are based on the NRG scenario, to first order it also mimics the NRH scenario, so that our comparison between MGRS and 2dFGRS applies to both cases.

Of the two scenarios illustrated in Fig. 6, the most likely one is the NRH scenario. It seems to fit naturally within a hierarchical picture of structure formation, where haloes

continue to grow in mass by accretion and merging. It is also in accord with our finding that b_{vel} is larger in more massive haloes, which form later and are thus expected to be less relaxed. A potential problem for this scenario, however, is the fact that in the Λ CDM concordance cosmology the growth rate of structures should drop fairly rapidly at the current epoch. Numerical simulations are ideally suited to investigate whether a value of $b_{\text{vel}} \simeq 0.5$ is a natural outcome of structure formation in the Λ CDM concordance cosmology or not. Using a combination of numerical simulations and semi-analytical models of galaxy formation in a Λ CDM cosmology, Diaferio et al. (1999) found that the central galaxy has an average velocity with respect to the halo barycenter of $\sim 80 \text{ km s}^{-1}$. With a median halo mass of $\sim 10^{13} h^{-1} M_{\odot}$, this corresponds to an average velocity bias of $b_{\text{vel}} \simeq 0.35$, in reasonable agreement with our results. Yoshikawa, Jing & Börner (2003) used a smoothed-particle hydrodynamics (SPH) simulation of galaxy formation in a Λ CDM universe, and found that the average velocity difference between the most massive halo galaxy and the mass center of the dark matter halo is $\langle v_c - v_{\text{dm}} \rangle \simeq 0.5 \langle \sigma_{\text{dm}} \rangle$ (see their Fig. 10)[§]. This is in excellent agreement with our best-fit value of $b_{\text{vel}} = 0.5$. These two simulations suggest that our results are in perfect accord with the Λ CDM concordance cosmology. Note, however, that Yoshikawa et al. (2003) did not investigate whether the most massive halo galaxy has a net velocity with respect to the most bound halo particle, while in Diaferio et al. (1999) the central galaxy is associated with the most bound halo particles by construction. Therefore, we not use either of these results to discriminate between the NRG and NRH scenarios.

The NRG scenario appears unlikely at first sight, as dynamical friction against the highly concentrated dark matter halo should quickly damp any oscillatory motion. On the other hand, if dark matter haloes are cored, rather than cusped, the oscillations may persist for a much longer time (cf. Bontekoe 1988). This possibility is interesting in light of various independent claims for cored dark matter haloes, based on rotation curves of dwarf and low surface brightness galaxies (e.g., Moore 1994; Flores & Primack 1994; Borriello & Salucci 2001; de Blok et al. 2001; de Blok & Bosma 2002, but see also van den Bosch et al. 1999; van den Bosch & Swaters 2001; Dutton et al. 2005), on the observed pattern speeds of barred galaxies (Debattista & Sellwood 1998, 2000), and on the longevity of the lopsidedness of disk galaxies (Levine & Sparke 1998). A more in-depth study of the damping rate of these kind of oscillations in dark matter haloes, both cusped and cored, could shed more light on these issues.

Independent of which of the aforementioned scenarios is responsible for the non-zero velocity bias of the brightest halo galaxies, it has important implications for various areas in astrophysics. First of all, it has an important impact on the use of satellite kinematics to infer halo masses. Since the number of detectable satellites in individual systems is generally small, one typically stacks the data on many host-satellite pairs to obtain *statistical* estimates of halo masses

[§] We assumed isotropy to convert the three-dimensional velocity dispersion of the dark matter particles quoted in Yoshikawa et al. (2003) to the one-dimensional velocity dispersion $\langle \sigma_{\text{dm}} \rangle$.

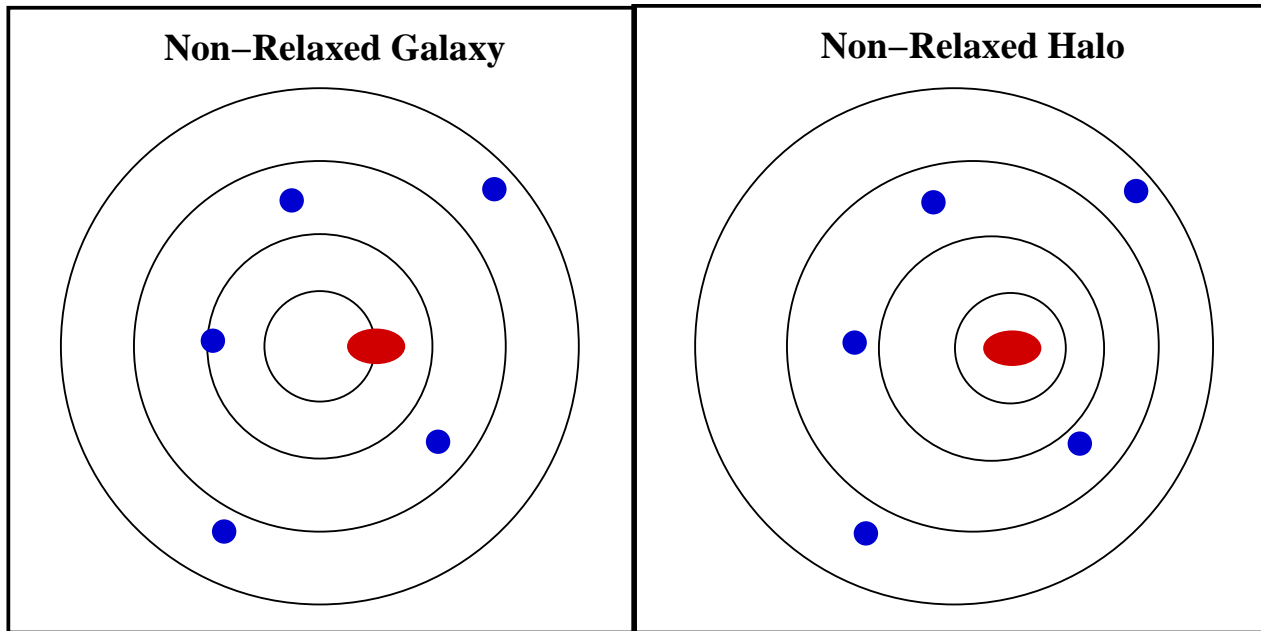


Figure 6. An illustration of the two different configurations that are both consistent with our inferred offset between the brightest halo galaxy and the satellite galaxies. Contours depict equipotentials of the dark matter haloes, while filled ellipses and circles represent brightest halo galaxies and satellite galaxies, respectively. In the Non-Relaxed Galaxy (NRG) scenario, the brightest halo galaxy oscillates in a fully relaxed halo. In the Non-Relaxed Halo (NRH) scenario, on the other hand, the central galaxy coincides with the minimum of the halo potential, but the centers of different equipotential surfaces are offset from each other. See text for a detailed discussion.

(Erickson, Gottesman & Hunter 1987; Zaritsky et al. 1993, 1997; Zaritsky & White 1994; McKay et al. 2002; Brainerd & Specian 2003; Prada et al. 2003; van den Bosch et al. 2004). The halo mass is typically derived from the dispersion, σ_{cs} , of the distribution of the velocity difference between host and satellite galaxies. This derivation rests on the (standard) assumptions that the host galaxies (i.e., the brightest halo galaxies) are at rest with respect to the center of a *relaxed* dark matter halo. If the satellite galaxies have the same kinematics as dark matter particles, then $\sigma_{cs} = \sigma_{dm} \propto M^{1/3}$. However, in the case of the NRH scenario, one simply can not use (satellite) kinematics to infer reliable halo masses, as the crucial assumption of a virialized system is not correct. In the case of the NRG scenario, on the other hand, the system is relaxed but, because of the non-zero velocity bias, we have that $\sigma_{cs} = \sqrt{1 + b_{vel}} \sigma_{dm}$. If one were not to correct for b_{vel} , the inferred halo mass will be overestimated by a factor $(1 + b_{vel})^{3/2}$ (corresponding to ~ 1.85 in the case of $b_{vel} = 0.5$).

The results presented here also have potentially important implications for (strong) gravitational lensing. In both the NRG and NRH scenarios one expects a strong, ‘external’ shear due to the dark matter halo, which should leave signatures in the image configurations and time delays of the lens. In fact, this ‘external’ shear may already have been detected. As shown in Keeton, Kochanek & Seljak (1997), fitting four-image lenses almost always requires an independent external shear that is not aligned with the light of the lens. Although this may reflect a misalignment between the luminous galaxy and dark matter halo, in agreement with the results presented here, there are alternative sources of external shear (nearby galaxies, large-scale structure along the line-of-sight) that may leave a similar signal in the lens

configuration. A more thorough, systematic study of multiply lensed systems is therefore required to put constraints on the spatial bias of brightest halo galaxies. In fact, strong gravitational lensing is probably the only method that can be used to detect an offset between halo and galaxy in *individual* systems, and to discriminate between the NRH and NRG scenarios.

A non-zero $\langle r_{cen} \rangle$ also impacts on the internal structure and dynamics of central galaxies. As the galaxy oscillates in the dark matter halo (NRG scenario), or the halo relaxes around the central galaxy (NRH scenario), it is constantly subjected to tidal forces that may trigger bar-instabilities in otherwise stable disks, and may create lopsidedness (Levine & Sparke 1998; Noordermeer, Sparke & Levine 2001). Detailed studies have revealed lopsidedness (either in the kinematics or the photometry) in about half of all disk galaxies studied (e.g., Richter & Sancisi 1994; Zaritsky & Rix 1997; Rudnick & Rix 1998; Haynes et al. 1998; Matthews, van Driel & Gallagher 1998; Swaters 1999). In fact, as shown by Bissantz, Englmaier & Gerhard (2003), the morphology and kinematics of gas in the inner few kpc of the Milky Way (in particular the 3kpc-arm) may indicate the presence of a similar $m = 1$ asymmetry in our own galaxy (cf. Fux 1999). The high frequency of lopsided and barred disk galaxies therefore seems to be in support of a non-zero $\langle r_{cen} \rangle$, whether it reflects a non-relaxed halo or a non-relaxed galaxy. Taking our results at face value, it is clear that any study of disk stability that ignores these strong distortions and time-variability of the potential may be missing an essential ingredient.

Finally, as mentioned in the introduction, a non-zero b_{vel} also plays a role in halo occupation models. Using the method described in detail in Yang et al. (2004), we com-

puted the projected two-point correlation function and pairwise peculiar velocity dispersions of MGRSs $M_{0.0}$, $M_{0.5}$, and $M_{1.0}$. The differences are found to be extremely small, well below the errors due to cosmic variance. Therefore, for all practical purposes, it suffices to model the phase-space parameters of galaxies in dark matter haloes with $b_{\text{vel}} = 0$ (as is generally done), when computing galaxy-galaxy correlation functions based on halo occupation distributions.

8 CONCLUSIONS

According to the standard paradigm of structure formation, the brightest galaxy in a dark matter halo should reside at rest at the center of the potential well. In order to test this ‘central galaxy paradigm’ (CGP), we used the halo-based galaxy group finder of Yang et al. (2005a) to construct group catalogues from the 2dFGRS and SDSS. For each group we compute the statistic \mathcal{R} , defined as the difference between the velocity of the brightest group galaxy and the average velocity of the other group members (satellites), normalized by the unbiased estimator of the velocity dispersion of the satellite galaxies. If the null-hypothesis of the CGP is correct, \mathcal{R} should follow a Student t -distribution. If, on the other hand, brightest halo galaxies have a non-zero velocity bias with respect to the satellite galaxies, the \mathcal{R} -distribution should be significantly broader. The applicability of this ‘ \mathcal{R} -test’ depends critically on how well one can group those galaxies that belong to the same dark matter halo. Although our group finder is well tested and calibrated, it is not perfect, and unavoidably selects interloper galaxies as group members. In addition, redshift surveys suffer from various incompleteness effects. We have shown that these effects result in a broadening of the \mathcal{R} -distribution, which, when not accounted for, may give the false impression that the CGP is ruled out.

In order to take interlopers and incompleteness effects into account, and thus allow for a fair comparison with the data, we construct detailed mock galaxy redshift surveys that can be compared with the 2dFGRS on a one-to-one basis. We apply our \mathcal{R} -statistic to the galaxy groups selected from these MGRS, which we compare to those obtained from the 2dFGRS using the Kolmogorov-Smirnov test. This shows that the CGP is inconsistent with the data at high confidence, and that instead the brightest halo galaxies have a specific kinetic energy that is about 25 percent of that of satellite galaxies. For a typical, relaxed, cold dark matter halo this corresponds to an expectation value for the offset between galaxy and halo of ~ 3 percent of the virial radius, comparable to the characteristic radius of the galaxy. In addition, we find a weak hint that the velocity bias of brightest halo galaxies is larger in more massive haloes.

We have focussed mainly on the \mathcal{R} -distributions obtained from the 2dFGRS, simply because we have accurate MGRSs available for this data set. However, we have shown that the \mathcal{R} -distributions obtained from groups in the SDSS are in excellent agreement with those obtained from the 2dFGRS, suggesting that the SDSS is also inconsistent with the CGP.

Undoubtedly, the most important implication of our results is the puzzling question as to the origin of the offset between the central galaxy and its satellites. Probably the

most likely explanation is that the majority of dark matter haloes are not yet fully relaxed. In this case, the brightest halo galaxy may still coincide with the *minimum* of the potential well, but that minimum does not coincide with the center of mass measured over the entire halo. Although this picture seems consistent with our finding that the specific kinetic energy of the brightest halo galaxies is larger in more massive haloes, which form later, detailed numerical simulations are required to investigate whether the typical growth rates of dark matter haloes are sufficiently large and violent to explain our findings in a Λ CDM concordance cosmology. A first hint that this is indeed the case comes from the simulations of Diaferio et al. (1999) and Yoshikawa et al. (2003), which reveal a velocity bias of brightest halo galaxies that is very similar to that found here. Although this suggests that a non-zero velocity bias is a natural outcome of structure formation in a Λ CDM cosmology, it still needs to be verified whether, in these simulations, the central galaxy is at rest with respect to the *minimum* of the potential well.

An alternative explanation for the non-zero velocity of the brightest halo galaxies with respect to the satellite galaxies may be that the halo is relaxed, but that the brightest halo galaxy oscillates in the central potential well. If the dark matter halo is strongly concentrated, as expected for typical cold dark matter haloes, one would naively expect that any such oscillation is quickly damped by dynamical friction. However, this damping timescale may be significantly longer if there is less dark matter in the center of the halo than anticipated; i.e., the density distribution is cored rather than cusped. This possibility is interesting in light of the recent claims for cored haloes based on the observed rotation curves and bar pattern speeds of disk galaxies.

In either case, the brightest halo galaxy is expected to experience a time-varying tidal field. This strongly questions the applicability of (numerical) studies of galaxy dynamics, and in particular of stability analyzes that make the assumption that the galaxy is at rest at the center of a relaxed dark matter halo. In particular, it may explain the high frequency and longevity of bars and lopsidedness in disk galaxies. The fact that we find evidence for a non-zero velocity of the brightest halo galaxy with respect to the satellite galaxies also has important implications for the determination of halo masses based on the kinematics of host-satellite systems, and for the modeling of strong gravitational lenses. For the purpose of computing galaxy-galaxy correlation functions based on halo occupation models, however, one can safely ignore the fact that the CGP does not hold, and make the simple ansatz that the brightest halo galaxy resides at rest at the halo center.

ACKNOWLEDGEMENTS

We are grateful to Michael Blanton for his help with the NYU-VAGC, and to Victor Debattista, Savvas Koushiappas, George Lake, Shude Mao, Ben Moore, Peter Schneider, Joachim Stadel, and Simon White for useful discussions.

REFERENCES

Abazajian K., et al., 2004, *AJ*, 128, 502

- Berlind A.A., Weinberg D.H., 2002, *ApJ*, 575, 587
- Binney J.J., Tremaine S.D., 1987, *Galactic Dynamics* (Princeton: Princeton Univ. Press)
- Bissantz N., Englmaier P., Gerhard O.E., 2003, *MNRAS*, 340, 949
- Blanton M.R., et al., 2004, preprint (astro-ph/0410166)
- Bontekoe T.R., 1988, Ph.D. Thesis, Groningen University
- Boriello A., Salucci P., 2001, *MNRAS*, 323, 285
- Brainerd T.G., Specian M.A., 2003, *ApJ*, 593, L7
- Cole S., Lacey C.G., Baugh C.M., Frenk C.S., 2000, 319, 168
- Cole S., The 2dFGRS team, 2001, *MNRAS*, 326, 255
- Colless M., The 2dFGRS team, 2001, *MNRAS*, 328, 1039
- Debattista V.P. Sellwood J.A., 1998, *ApJ*, 493, L5
- Debattista V.P. Sellwood J.A., 2000, *ApJ*, 543, 704
- de Blok W.J.G., McGaugh S.S., Bosma A., Rubin V.C., 2001, *ApJ*, 552, L23
- de Blok W.J.G., Bosma A., 2002, *A&A*, 385, 816
- Diaferio A., Kauffmann G., Colberg J.M., White S.D.M., 1999, *MNRAS*, 307, 537
- Dutton A.A., Courteau S., de Jong R.S., Carignan C., 2005, *ApJ*, 619, 218
- Eke V.R., Navarro J.F., Steinmetz M., 2001, *ApJ*, 554, 114
- Erickson L.K., Gottesman S.T., Hunter J.H., 1987, *Nature*, 325, 779
- Flores R.A., Primack J.R., 1994, *ApJ*, 427, L1
- Fux R., 1999, *A&A*, 345, 787
- Hawkins E., The 2dFGRS team, 2003, *MNRAS*, 346, 78
- Haynes M.P., Hogg D.E., Maddalena R.J., Roberts M.S., van Zee L., 1998, *AJ*, 115, 62
- Hernquist L., 1990, *ApJ*, 356, 359
- Hill J.M., Hintzen P., Oegerle W.R., Romanishin W., Lesser M.P., Eisenhamer J.D., Batuski D.J., 1988, *ApJ*, 332, L23
- Jing Y.P., Suto, Y., 2002, *ApJ*, 574, 538
- Jones C., Mandel E., Schwarz J., Forman W., Murray S.S., Harnnden F.R., 1979, *ApJ*, 234, L21
- Kauffmann G., White S.D.M., Guiderdoni B., 1993, *MNRAS*, 264, 201
- Keeton C.R., Kochanek C.S., Seljak U., 1997, *ApJ*, 482, 604
- Levine S.E., Sparke L.S., 1998, *ApJ*, 496, L13
- Madgwick D.S., The 2dFGRS team, 2002, *MNRAS*, 333, 133
- Magliocchetti M., Porciani C., 2003, *MNRAS*, 346, 186
- Matthews L.D., van Driel W., Gallagher J.S., 1998, *AJ*, 116, 1169
- McKay T.A. et al., 2002, *ApJ*, 571, L85
- Moore B., 1994, *Nature*, 370, 629
- Mulchaey J.S., Zabludoff A.I., 1998, *ApJ*, 496, 73
- Navarro J.F., Frenk C.S., White S.D.M., 1997, *ApJ*, 490, 493
- Noordermeer E., Sparke L.S., Levine S.E., 2001, *MNRAS*, 328, 1064
- Norberg P., The 2dFGRS team, 2002, *MNRAS*, 336, 907
- Oegerle W.R., Hill J.M., 1994, *AJ*, 107, 857
- Oegerle W.R., Hill J.M., 2001, *AJ*, 122, 2858
- Postman M., et al., 1996, *AJ*, 111, 615
- Prada F., et al., 2003, *ApJ*, 598, 260
- Quintana H., Lawrie D.G., 1982, *AJ*, 87, 1
- Richter O.-G., Sancisi R., 1994, *A&A*, 290, L9
- Rudnick G., Rix H.-W., 1998, *AJ*, 116, 1163
- Scoccimarro R., Sheth R.K., Hui L., Jain B., 2001, *ApJ*, 546, 20
- Sharples R.M., Ellis R.S., Gray P.M., 1988, *MNRAS*, 231, 479
- Sheth R.K., Mo H.J., Tormen G., 2001, *MNRAS*, 323, 1
- Somerville R.S., Primack J.R., 1999, *MNRAS*, 310, 1087
- Swaters R.A., 1999, Ph.D. Thesis, Groningen University
- Tinker J., Weinberg D.H., Zheng Z., Zehavi I., 2004, preprint (astro-ph/0411777)
- van den Bosch F.C., Robertson B.E., Dalcanton J.J., de Blok W.J.G., 1999, *AJ*, 119, 1579
- van den Bosch F.C., Swaters R.A., 2001, *MNRAS*, 325, 1017
- van den Bosch F.C., Yang X., Mo H.J., 2003, *MNRAS*, 340, 771
- van den Bosch F.C., Norberg P., Mo H.J., Yang X., 2004, *MNRAS*, 352, 1302
- van den Bosch F.C., Mo H.J., Yang X., Norberg P., 2005, *MNRAS*, 356, 1233
- White S.D.M., Rees M.J., 1978, *MNRAS*, 183, 341
- Yang X., Mo H.J., van den Bosch F.C., 2003, *MNRAS*, 339, 1057
- Yang X., Mo H.J., Jing Y.P., van den Bosch F.C., Chu Y., 2004, *MNRAS*, 350, 1153
- Yang X., Mo H.J., van den Bosch F.C., Jing Y.P., 2005a, *MNRAS*, 356, 1293 (YMBJ)
- Yang X., Mo H.J., van den Bosch F.C., Jing Y.P., 2005b, *MNRAS*, 357, 608
- Yang X., Mo H.J., Jing Y.P., van den Bosch F.C., 2005c, *MNRAS*, in press (astro-ph/0410114)
- York D., et al., 2000, *AJ*, 120, 1579
- Yoshikawa K., Jing Y.P., Börner G., 2003, *ApJ*, 590, 654
- Zabludoff A.I., Huchra J.P., Geller M.J., 1990, *ApJS*, 74, 1
- Zabludoff A.I., Mulchaey J.S., 1998, *ApJ*, 496, 39
- Zaritsky D., Smith R., Frenk C.S., White S.D.M., 1993, *ApJ*, 405, 464
- Zaritsky D., White S.D.M., 1994, *ApJ*, 435, 599
- Zaritsky D., Smith R., Frenk C.S., White S.D.M., 1997, *ApJ*, 478, 39
- Zaritsky D., Rix H.W., 1997, *ApJ*, 477, 118
- Zehavi I., et al., 2004, preprint (astro-ph/0408569)
- Zheng Z., et al., 2004, *ApJ*, preprint (astro-ph/0408564)